Heliyon 9 (2023) e23091

Contents lists available at ScienceDirect

Heliyon

journal homepage: www.cell.com/heliyon

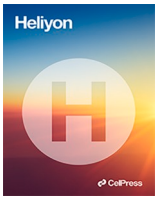

Polyelectrolyte-based solid dispersions for enhanced dissolution and pH-Independent controlled release of sildenafil citrate

Ju-Hyeong Woo [a,1], Hai V. Ngo [a,1], Hy D. Nguyen [a], Myung-Chul Gil [a], Chulhun Park [b], Jun-Bom Park [c], Jing-Hao Cui [d], Qing-Ri Cao [d], Beom-Jin Lee [a,e,*]

[a] College of Pharmacy, Ajou University, Suwon 16499, Republic of Korea
[b] College of Pharmacy, Jeju National University, Jeju 63243, Republic of Korea
[c] College of Pharmacy, Sahmyook University, Seoul 01795, Republic of Korea
[d] College of Pharmaceutical Sciences, Soochow University, Suzhou 215123, China
[e] Institute of Pharmaceutical Science and Technology, Ajou University, Suwon 16499, Republic of Korea

ARTICLE INFO

Keywords:
Sildenafil citrate
Soluplus®-based solid dispersion
Enhanced dissolution
Differently charged polymers
Polyelectrostatic interaction
Controlled release

ABSTRACT

The aim of this study was to design a novel matrix tablet with enhanced dissolution and pH-independent controlled release of sildenafil citrate (SIL), a drug with pH-dependent solubility, by using solid dispersions (SDs) and polyelectrostatic interactions. SIL-loaded SDs were prepared using various polymeric carriers such as poloxamer 188, poloxamer 407, Soluplus®, polyvinylpyrrolidone (PVP) K 12, and PVP K 17 by the solvent evaporation method. Among these polymers, Soluplus® was found to be the most effective in SDs for enhancing the drug dissolution over 6 h in pH 6.8 intestinal fluid. SIL was well dispersed in Soluplus®-based SDs in an amorphous form. When the Soluplus®-based SDs were added in the tablet containing positively charged chitosan and negatively charged Eudragit® L100, the drug release rate was further modulated in a controlled manner. The charge density of the tablet was higher at pH 6.8 than at pH 1.2 due to the polyelectrostatic interaction between chitosan and Eudragit® L100. This interaction could provide a pH-independent controlled release of SIL. Our study demonstrates that a combinatory approach of Soluplus®-based SDs and polyelectrostatic interactions can improve the dissolution and pH-independent release performance of SIL. This approach could be a promising pharmaceutical strategy to design a matrix tablet of poorly water-soluble drugs for the enhanced bioavailability.

1. Introduction

Pulmonary arterial hypertension (PAH) is defined as a disease of the small pulmonary arteries characterized by vascular remodeling and proliferation [1]. It results in a progressive increase in pulmonary vascular resistance and pulmonary pressure, ultimately leading to reduced cardiac output, right ventricular failure, and death [2]. Sildenafil citrate (SIL) has been prescribed for the treatment of erectile dysfunction and PAH due to its ability to stimulate cyclic guanosine monophosphate-mediated growth inhibition and the relaxation of vascular smooth muscle in the lung [3]. SIL is a basic drug absorbed mainly from the intestine, where its solubility is

* Corresponding author. College of Pharmacy, Ajou University, Suwon 16499, Republic of Korea.
E-mail address: bjl@ajou.ac.kr (B.-J. Lee).
[1] Equally contributed.

https://doi.org/10.1016/j.heliyon.2023.e23091
Received 8 August 2023; Received in revised form 12 November 2023; Accepted 27 November 2023
Available online 30 November 2023

limited (0.4 mg/mL at pH 6.8) [4]. In addition, SIL has a short half-life (4 h) and low oral bioavailability (38–42 %), therefore PAH patients are required to take 20 mg tablets three times daily, resulting in adverse effects such as the fluctuations of plasma drug concentrations and unwanted dose-related side effects, reducing patient compliance [5]. Thus, it was motivated to design a new SIL-loaded matrix tablet formulations to simultaneously achieve enhanced dissolution rate and sustained release of poorly water-soluble SIL in a pH-independent manner [6,7]. The physicochemical properties of SIL are given in Table 1.

To enhance the dissolution of SIL, different techniques have been investigated in previous studies, such as salt and cocrystals with dicarboxylic acids [8], incorporation of superdisintegrant [9], self-nanoemulsifying drug delivery system, amorphous microspheres, crystalline microspheres [10], cyclodextrin complex [11], and solid dispersion (SD) [12]. Among them, SD has gained significant attention for its effectiveness in improving the dissolution and bioavailability of SIL. Different types of hydrophilic carriers such as β-cyclodextrin, polypropylene glycol, and PVP K30 were used to prepare SDs [12–14]. In our study, we extended this approach using various hydrophilic polymers including poloxamer 188, poloxamer 407, Soluplus®, PVP K 12, and PVP K 17 to prepare SIL-loaded SDs through the solvent evaporation method, aimed at enhancing the dissolution rate of SIL at pH 6.8 upon the benefits of SD technology. Due to the variations in the melting points of different polymers, solvent evaporation method was considered as a preferable choice to prepare SIL-loaded SDs. The physicochemical properties of SIL-loaded SDs were characterized by scanning electron microscopy (SEM), particle size distribution, high powder X-ray diffraction (PXRD) and differential scanning calorimetry (DSC).

When the dissolution of SIL was improved, SD-loaded matrix tablets using differently charged polymers were prepared by direct compression to utilize their polyelectrostatic interactions for the pH-independent controlled release of SIL. In this study, two polymers, chitosan and Eudragit® L 100 with different charges were chosen to prepare matrix tablet containing SIL-loaded SDs. Chitosan is a cationic linear polymer consisting of β (1 → 4)-linked D-glucosamine (the deacetylated unit) and N-acetyl-D-glucosamine (the acetylated unit) [15]. It has good solubility in acidic solutions (pH < 6) owing to the primary amine groups (pKa = 6.3), which become protonated in acidic conditions [16]. Subsequently, the positively charged chitosan polymer can swell from the uptake of water, and this swelling effect retards the drug release [17]. On the other hand, Eudragit® L100 is an anionic copolymer composed of methyl methacrylate and methacrylic acid. At a pH of above 6.0, the carboxylic acid groups lose their protons, and the polymer becomes negatively charged [18]. The negatively charged Eudragit® L100 can form polyelectrostatic complexes with poly-cationic polymers. Therefore, chitosan and Eudragit® L 100 can be used to prepare a polyelectrostatic matrix tablet containing SIL-loaded SDs for the purpose of modulating the release rate of poorly water-soluble SIL in a controlled manner. The release rate of matrix tablets containing SIL-loaded SDs were then investigated in pH 1.2 gastric fluid for 2 h followed by pH 6.8 intestinal fluid for 22 h [7].

2. Materials and methods

2.1. Materials

SIL, microcrystalline cellulose 101 (MCC 101), polyvinylpyrrolidone K 30 (PVP K 30), chitosan, magnesium stearate, and Viagra® tablets were obtained from Korea United Pharm. Inc. (Seoul, Korea). Poloxamer 188, poloxamer 407, Soluplus®, PVP K 12, PVP K 17, and polyethylene glycol 6000 (PEG 6000) were purchased from BASF Co., Ltd (Heidelberg, Germany). Eudragit® L 100 was purchased from Evonik Industries AG (Darmstadt,Germany).

2.2. Preparation of SIL-loaded SDs

First, 3 g and 6 g of each of poloxamer 188, poloxamer 407, Soluplus®, PVP K 12, PVP K 17, and polyethylene glycol 6000 (PEG 6000) were placed in each beaker and dissolved in an adequate amount of ethanol. Subsequently, 3 g SIL was added to each beaker. The solution was stirred at 500 rpm for 30 min by using a magnetic bar and dried for 24 h in a vacuum dryer. The dried powder was ground with a blender and cooled; this process was repeated five times, and the powder was then passed through a 140-mesh sieve. The

Table 1
Physicochemical properties of SIL.

Factor	Property
Indication	Erectile dysfunction Pulmonary arterial hypertension
Chemical formula	$C_{28}H_{38}N_6O_{11}S$
Molecular weight	666.7 g/mol
Melting point	190 °C
Bioavailability	41 %
Dose	50, 100 mg qd (Erectile dysfunction) 20 mg tid (Pulmonary arterial hypertension)
Major absorption	Jejunum, duodenum (pH = 6–7)
pK_a	5.97
Protein binding	96 %
Half life	4 h
State	Solid, white powder
Solubility	37.25 mg/mL (at pH 1.2) 0.4 mg/mL (at pH 6.8)

formulation composition of the SIL-loaded SDs at two different ratios (SIL:polymeric carrier = 1:1 or 1:2) is given in Table 2.

2.3. Characterization of SIL-loaded SDs

2.3.1. Scanning electron microscopy (SEM)

The morphology of SIL-loaded SDs was examined by using a Jeol JSM-7900F (Akishima, Japan) scanning electron microscope at a voltage of 2 kV. The samples were mounted on the brass stage by using carbon tape and coated with gold-palladium for 90 s under an argon atmosphere by using an automatic sputter coater.

2.3.2. Particle size distribution

The particle size distribution of SIL-loaded SDs was investigated using HELOS & RODOS (Sympatec GmBH, Germany) with a spectrum range R5 (from 0.5 to 875 μM). First, weigh 1 mg of samples each other, and then, placed samples on the dry dispersion with 100 m/s of exit speed.

2.3.3. High powder X-ray diffraction (PXRD)

SIL-loaded SDs were analyzed by PXRD with D/max-2500V/PC (Rigaku, Japan) using Cu-K_α radiation at 40 kV and 50 mA. The samples were scanned from 2° to 60° (diffraction angle, two-theta) with a rate of change in the diffraction angle of 0.02°/s.

2.3.4. Differential scanning calorimetry (DSC)

The thermal behavior of SIL-loaded SDs was investigated by using a DSC 200 F3 Maia (Netzsch, Germany). First, 5 mg of each sample was weighed on the standard open aluminum pan, with an empty open aluminum pan used as a reference. Each sample was heated from 5 °C to 250 °C at a rate of temperature 10 °C/min, with nitrogen gas used for the purge process. The calibration of temperature and heat flow was performed by using indium.

2.4. Preparation of matrix tablets containing SIL-loaded SDs

The formulation compositions of the polyelectrostatic matrix tablets containing Soluplus®-based SIL-loaded SDs are listed in Table 3. Tablets were made by using the direct compression method. Soluplus®-based SDs and other excipients, except for the magnesium stearate, were mixed thoroughly with a blender and cooled. The mixing and cooling procedures were repeated five times. Finally, magnesium stearate was added as a lubricant, and the mixture was mixed thoroughly with a blender and cooled; again, the mixing and cooling procedures were repeated five times. The mixture was passed through a 140-mesh sieve to obtain the final powder, which was then directly compressed in a single punch tablet press (DCM Korea Co., Gimpo, Korea). The cylindrical matrix tablets containing SIL-loaded SDs had the following characteristics: diameter; 13 mm, hardness; 25 ± 5 N.

2.5. Polyelectrostatic interactions between chargeable polymers

To check and understand molecular interaction using Fourier-transform infrared (FT-IR) between drug and two model polymers, drug-loaded dried powders in polymer (chitosan + SIL, Eudragit® L 100 + SIL and chitosan + Eudragit® L 100 + SIL) and polyelectrostatic complexes without drug (chitosan and Eudragit® L 100) were used. Drug-loaded dried powders were prepared by vacuum-drying the pH 6.8 buffer solution including drug and excipients at a ratio of 1:1 or 1:1:1. In addition, polyelectrostatic complexes were prepared by vacuum drying the pH 6.8 buffer solution including chitosan and Eudragit® L 100 in a ratio of 1:1.

The FT-IR absorption spectrum of the samples was obtained by using an FT-IR spectrophotometer (Nicolet iS50, Thermo Fisher Scientific, Madison, WI, USA). The variation in adsorption peaks was scanned from 400 to 2000 cm^{-1} at a resolution of 0.5 cm^{-1}.

2.6. Drug release from SIL-loaded SDs and matrix tablets

The dissolution test of SIL-loaded SD was performed using a D-TWELVE dissolution tester (DCM Korea Co., Gimpo, Korea) and dissolution apparatus II (paddle apparatus, speed; 50 rpm, volume; 900 mL of pH 6.8 buffer, temperature; 37 °C ± 0.5 °C) to determine the optimal formulation for 6 h.

Table 2
Formulation compositions (mg) of SIL-loaded SDs.

Composition	SD1	SD2	SD3	SD4	SD5	SD6	SD1-1	SD2-1	SD3-1	SD4-1	SD5-1	SD6-1
SIL	84.3	84.3	84.3	84.3	84.3	84.3	84.3	84.3	84.3	84.3	84.3	84.3
Poloxamer 188	168.6	–	–	–	–	–	84.3	–	–	–	–	–
Poloxamer 407	–	168.6	–	–	–	–	–	84.3	–	–	–	–
Soluplus®	–	–	168.6	–	–	–	–	–	84.3	–	–	–
PVP K 12	–	–	–	168.6	–	–	–	–	–	84.3	–	–
PVP K 17	–	–	–	–	168.6	–	–	–	–	–	84.3	–
PEG 6000	–	–	–	–	–	168.6	–	–	–	–	–	84.3
Total weight	252.9	252.9	252.9	252.9	252.9	252.9	168.6	168.6	168.6	168.6	168.6	168.6

Table 3
Formulation composition (mg) to prepare controlled release matrix tablet (500 mg total weight) using differently charged polymers and SIL-loaded SDs (SD3).

Composition	F1	F2	F3
SD3[a]	252.9	252.9	252.9
Chitosan	50	–	25
Eudragit® L 100	–	50	25
MCC 101	182.1	182.1	182.1
PVP K 30	10	10	10
Magnesium stearate	5	5	5
Total weight	500	500	500

[a] SD3: Soluplus®-based solid dispersion containing 83.4 mg SIL and 168.6 mg Soluplus®.

The dissolution rate of polyelectrostatic matrix tablet containing Soluplus®-based SIL-loaded SDs was tested by switching method in the pH 1.2 buffer for 2 h followed by pH 6.8 buffer for 22 h. After testing for 2 h in the pH 1.2 buffer, the remaining drug samples were collected from the vessel using the spatula, and then vacuum-filtered using the membrane filter paper. The resulting samples were then poured to pre-warmed dissolution media (volume; 900 mL pH 6.8 buffer, temperature; 37 °C ± 0.5 °C) to resume release test for 22 h.

Throughout the test, 3 mL samples were withdrawn and replaced by the same volume of fresh pH 1.2 or pH 6.8 buffer to ensure a constant dissolution volume (900 mL) after each collection. The samples were filtered through a 0.45 μM PVDF syringe membrane filter. All dissolution tests were performed three times.

2.7. Charge density (CD) analysis

In order to examine chargeable behaviors, different formulations (SD3, F1, F2, and F3) were tested in the same conditions as in the dissolution test. At different intervals of time, each sample was collected and injected to the Charge Analyzing System (CAS-II Touch, Leipzig, Germany) to determine the charge density of the solution [19]. 0.01 N poly-diallyl-dimethyl-ammonium chlorides and 0.01 N poly-vinylsulfonic acid (sodium salt) were utilized as standard cationic and anionic titrants, respectively, with a resolution of 1 μL. Triplicate measurements were performed for each sample.

2.8. HPLC analysis

The HPLC system (Waters Alliance 2690, Waters Co., Ltd., Milford, MA, USA) consisted of a pump, a UV–visible spectrophotometric detector (Waters 2487 dual absorbance detector), a reverse column (HyPurity ™ C18 column, 250 × 4.6 mm, Thermo Scientific™), and an integrator (Empower Pro software version 5.0). The concentration of SIL was calculated from the detection of the absorption at a wavelength of 225 nm. The mobile phase was composed of a 40:60 (v/v) mixture of buffer (8.70 g of K_2HPO_4 in 1000 mL distilled water) and acetonitrile [20]. The mobile phase was degassed under a sonicator for 30 min and then filtered through a 0.45 μM PTFE membrane filter. The flow rate and column temperature were set to 1 mL/min and 25 °C respectively; 10 μL of each sample as injected

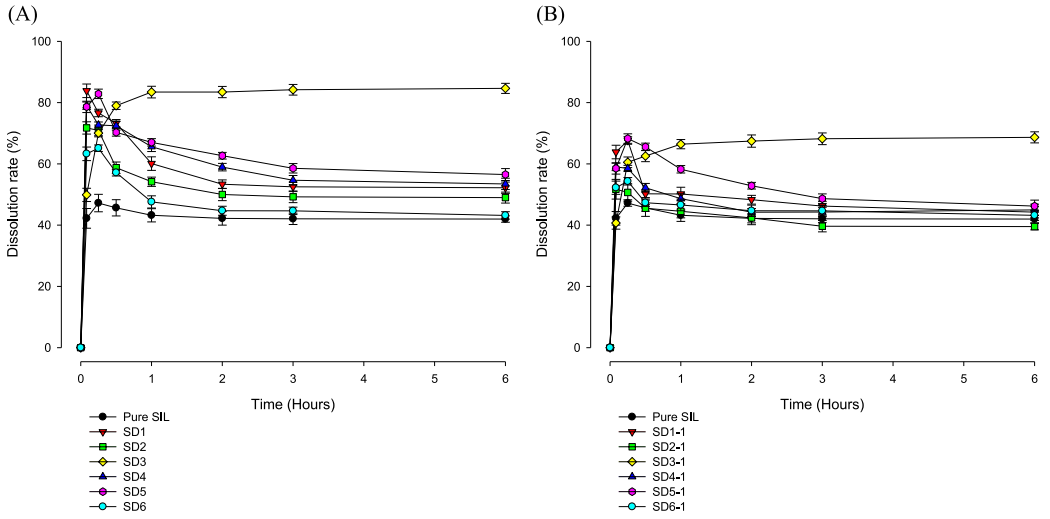

Fig. 1. Effect of polymeric carriers on the dissolution rate of SIL in binary solid dispersions at pH 6.8 intestinal fluid (n = 3). (A) SIL:polymeric carrier = 1:2, (B) SIL:polymeric carrier = 1:1.

into the HPLC, and the analysis time was 10 min.

3. Results and discussion

3.1. Dissolution rate of SIL-loaded SDs

The effect of six polymeric carriers on the dissolution rate of SIL in binary SDs at pH 6.8 intestinal fluid is shown in Fig. 1. The dissolution rate of pure SIL reached up to approximately 50 % at 15 min, and then decreased, showing spring-like precipitation. All SIL-loaded SDs showed a higher initial dissolution rate than pure SIL. As the ratio of polymeric carrier increased from 1:1 to 1:2, the initial dissolution rate was also increased accordingly. However, all SIL-loaded SDs showed a sudden decrease in dissolution rate with spring-like precipitation, except for Soluplus® -based SD3 or SD3-1 due to the supersaturation of SIL in media.

SIL-loaded SD3 using Soluplus® as a polymeric carrier, showed the most enhanced dissolution rate, approximately twice (~85 %) that of pure SIL. Furthermore, SIL-loaded SDs using Soluplus® did not show any of the precipitation behaviors that are commonly observed in SD systems owing to the supersaturation of drugs. Soluplus showed highly enhanced dissolution of SIL to suppress re-crystallization by maintaining supersatutation, mainly in pH 6.8 solution that drug has limited solubility. Therefore, Soluplus® was chosen as an optimal polymeric carrier for the preparation of SIL-loaded SDs.

3.2. Physicochemical characterization of SIL-loaded SDs

The surface morphology of SIL, Soluplus®, a physical mixture of SIL and Soluplus®, and six different types of SIL-loaded SDs using SEM is shown in Fig. 2. The SIL-loaded SDs showed a roughly round shape, whereas pure SIL showed an acicular shape that was characterized by a crystal form [21]. The physical mixture of SIL and Soluplus® contained two kinds of structure: an acicular shape from SIL and a round shape from Soluplus®. The acicular form of pure SIL was lost in the SIL-loaded SDs because SIL was well dispersed and present in an amorphous form.

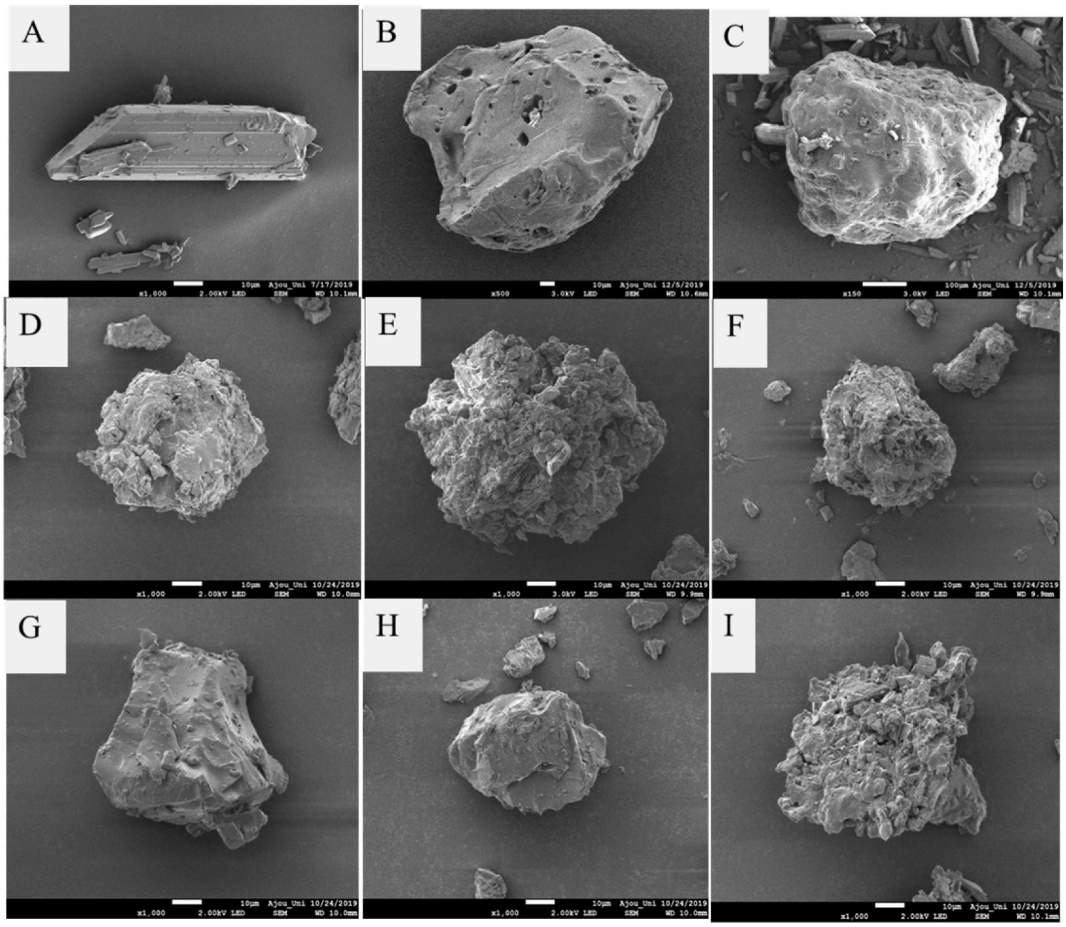

Fig. 2. SEM images of SIL (A), Soluplus® (B), (C) physical mixture of SIL and Soluplus® (C) and six different types of SIL-loaded SDs (D ~ I).

The median particle size of pure SIL and SIL-loaded SDs is reported in Table 4. The median particle size of the pure drug was only 9.13 μm, but that of SIL-loaded SDs was from 20.62 to 55.24 μm owing to the formation of agglomerated bulky particles. This suggested that SIL was well dispersed with the other polymeric solubilizers. Among them, Soluplus® resulted in the smallest particle size of the SIL-loaded SDs.

Any diffraction and peaks in PXRD and disappearance of intrinsic peak in DSC were qualitatively checked for amorphousness of SIL-loaded SDs because Soluplus® is mainly an amorphous carrier. The PXRD patterns of SIL, Soluplus®, a physical mixture of SIL and Soluplus®, and six different types of SIL-loaded SDs are shown in Fig. 3. The PXRD pattern of pure SIL showed the crystal form, as indicated by distinctive peaks at 8.32°, 10.50°, 14.64°, and 20.04°, respectively. However, the PXRD pattern of SIL-loaded SDs indicated only a small amount of the distinctive peaks of pure SIL. In particular, when compared with a physical mixture of SIL and Soluplus®, it was confirmed that SD3 had lower levels of the characteristic peaks of pure SIL. The reduction in peak size indicated that the drug was well dispersed in the polymeric carriers and formed an amorphous structure within the SIL-loaded SDs [6].

The DSC thermograms of pure SIL, pure Soluplus®, a physical mixture of SIL and Soluplus®, and six different types of SIL-loaded SDs are shown in Fig. 4. The glass transition temperature (T_g) is one of the most important properties of SIL-loaded SD and is the temperature region where the polymer transitions from a hard, glassy material to a soft, rubbery material. The T_g of a material characterizes the range of temperatures over which this glass transition occurs. The DSC thermogram of pure SIL had a sharp endothermal peak at 202.3 °C. When SIL was incorporated into SDs, a very weak endothermic peak was observed in the SIL-loaded SDs or the endothermal peak position of SIL-loaded SDs was shifted to a lower temperature as compared to the endothermic peak of pure SIL, indicating that there was a transformation of crystal habits of drug in SDs. As compared to pure SIL, the physical mixture of SIL and Soluplus® still remained a characteristic thermal peak of SIL at 202.3 °C. Interesting, in the preparation of SD3, the disappearance of intrinsic peak of SIL in DSC thermogram suggested there was a transition of drug crystal habit into amorphous state when the drug was incorporated into an amorphous Soluplus® carrier, which is in agreement to the PXRD analysis. As a conclusion, SIL was well dispersed in solid dispersions and present in a partially amorphous form.

3.3. FT-IR spectrometry

The FT-IR analysis of chitosan, Eudragit® L 100, SIL, dried powders (chitosan + SIL, Eudragit® L 100 + SIL, and chitosan + Eudragit® L 100 + SIL), and the polyelectrostatic complexes between chitosan and Eudragit® L 100 are shown in Fig. 5. In the spectrum of chitosan, the band situated at 1647 cm^{-1} was assigned to the amine N–H bending [22] and the characteristic peak of Eudragit® L 100 at 1704 cm^{-1} was assigned to the C═O stretching vibration of carboxylic groups [23]. In the spectrum of SIL, the band at 1357 cm^{-1} was assigned to S═O stretching of sulfonamide, and the band at 1171 cm^{-1} was assigned to C–N stretching of the amines [24].

The spectrum of dried powder containing SIL and Eudragit® L 100 contained a new peak at 1540 cm^{-1}, which was assigned to the N–O stretching of the nitro compound. The dried powder containing SIL, chitosan, and Eudragit® L 100 contained a similar new peak at 1542 cm^{-1}, which also was assigned to the N–O stretching of the nitro compound. However, the dried powder containing SIL and chitosan did not show a new peak in the N–O stretching range of the nitro compound (1550–1500 cm^{-1}) [25]. This new peak may be attributable to the interaction between the protonated amine groups ($–NH_3^+$) of SIL and the ionized carboxylic groups ($–COO^-$) of Eudragit® L 100 by polyelectrostatic interaction [26]. SIL and chitosan have the same (positive) charge, and therefore did not show an attractive interaction, but a repulsive interaction [27].

In the spectrum of polyelectrostatic complexes between chitosan and Eudragit® L 100, the amine N–H bending peak of chitosan disappeared, and the C═O stretching peak of the carboxylic groups of Eudragit® L 100 was present at a decreased level and was slightly moved to 1708 cm^{-1}. However, the new peak at 1547 cm^{-1} was observed, which was assigned to the N–O stretching of the nitro compound. This new peak may be attributable to the interaction between the protonated amine groups ($–NH_3^+$) of chitosan and the ionized carboxylic groups ($–COO^-$) of Eudragit® L 100 by polyelectrostatic interaction [28]. These results were very similar to polyelectrostatic complexes between xanthan gum containing carboxylic groups and chitosan [29].

3.4. Modulation of drug release from polyelectrostatic matrix tablets

Comparative release profiles of SIL-loaded SD3 and polymeric-based matrix tablets via polyelectrostatic interaction of differently charged polymers is shown in Fig. 6. It is known that pure SIL is completely dissolved after 5 min at pH 1.2, but is very limitedly released in pH 6.8 intestinal fluid [30]. SD3 powder and Viagra® tablet showed approximately 95 % and 97 % dissolution, respectively, at pH 1.2 for 2 h, and F2 showed a dissolution rate of 15 % lower than F1 and F3. The polymeric matrix tablet containing Soluplus®-based SDs showed a retarded release rate. Chitosan swelled under acidic conditions to form a positively charged hydrogel. In contrast, Eudragit® L100 was ionized and dissolved to form a negatively charged structure only above pH 6.0. Therefore, the positively charged chitosan (F1) yielded a much faster release rate compared with the negatively charged Eudragit® L100 (F2) with a

Table 4
Particle size distribution (μm) of SIL and SIL-loaded SDs (n = 3).

	SIL	SD1	SD2	SD3	SD4	SD5	SD6
Median (X_{50})	9.13 ±0.35	46.25 ±0.57	31.04 ±0.48	20.62 ±0.29	55.24 ±0.32	45.91 ±0.64	36.22 ±0.71

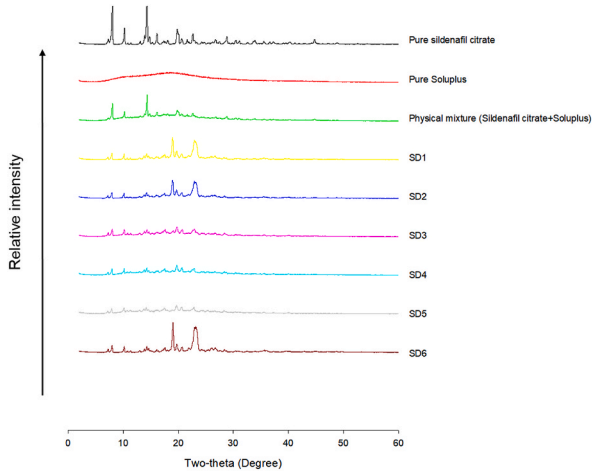

Fig. 3. PXRD patterns of SIL (A), Soluplus® (B), (C) physical mixture of SIL and Soluplus® (C) and six different types of SIL-loaded SDs (D ~ I).

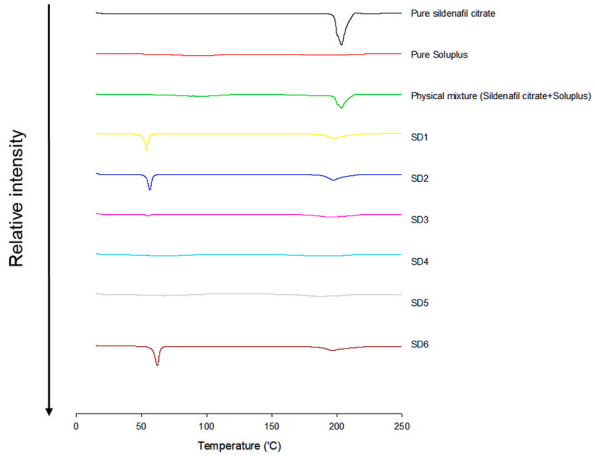

Fig. 4. DSC thermograms of SIL (A), Soluplus® (B), (C) physical mixture of SIL and Soluplus® (C) and six different types of SIL-loaded SDs (D ~ I).

cationic model drug via repulsive or attractive interaction.

After shifting pH 6.8 solution that SIL had limited solubility, SD3 powder maintained a similar dissolution rate of approximately 95 % within 24 h, whereas Viagra® tablet showed a slightly decreased dissolution rate of approximately 85 % at 24 h. The maximum dissolution occurred of F1 was reached a plateau at 14 h. Subsequently, the same dissolution rate was maintained, of approximately 90 % over 24 h. Like F1, F2 showed a gradual increase in dissolution rate to 14 h, but only reached 55 % dissolution, and a similar dissolution rate was maintained to approximately 60 % until 24 h. F2 had a barrier to drug release because the disintegration process was not completed over within 24 h, and it formed polyelectrostatic interactions between the positively charged SIL and the negatively charged Eudragit® L 100 to retard the dissolution rate of the drug. In contrast, the Soluplus®-based SD-loaded matrix tablet with polyelectrostatic complexes (F3) of chitosan and Eudragit® L 100 showed a steady modulation of drug release up to 24 h. The drug release rate was approximately 90 % at 24 h. The dissolution of polyelectrostatic complexes (F3) could vary according to the ratio of chitosan and Eudragit® L100 and was ranged between 100 % chitosan and 100 % Eudragit® L100.

In the pH 6.8 condition, chitosan (pKa = 6.3) remains polycation and Eudragit® L 100 (pKa = 4.0, carboxylic acid part) remains polyanion. Chitosan is expected to be predominately in the unionized form at pH 6.8 solution by Henderson-Hasselbach equation, but a gradual chemical interaction is occurred to produce ionic complex between chitosan and Eudragit® L 100. It is very unlikely to form the likelihood of phosphate ($H_2PO_4^{2-}$) ionic aggregate or complex with chitosan to retard the drug release because $H_2PO_4^{2-}$ molecular weight is very small (about 96.98 g/mol). In contrast, Eudragit L 100 is polymer (mw, about 125,000 g/mol) so it can make physical barrier with chitosan by ionic complex to delay the drug release. The formation of polyelectrostatic complexes between chitosan and Eudragit® L 100 may play a key role in the gradual retardation of drug release at pH 6.8 up to 24 h, suggesting it is suitable for a once-daily formulation for the treatment of pulmonary arterial hypertension.

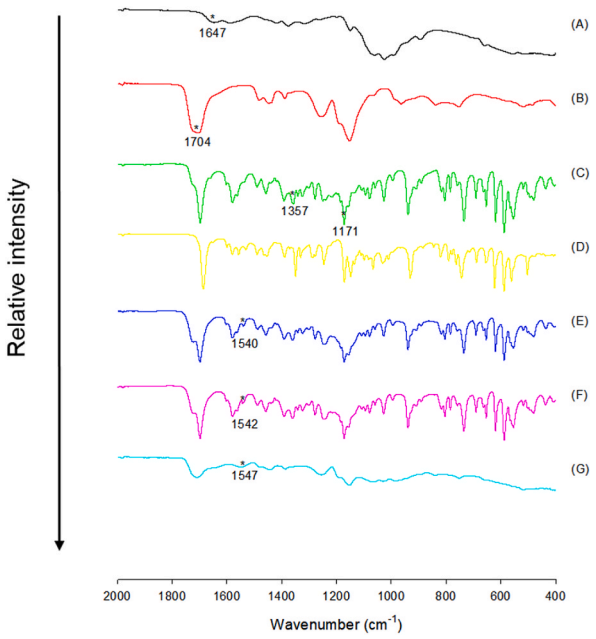

Fig. 5. FT-IR spectrum of (A) chitosan, (B) Eudragit® L 100, (C) SIL, (D) Chitosan + SIL, (E) Eudragit® L 100 + SIL, (F) Chitosan + Eudragit® L 100 + SIL, and (G) the polyelectrostatic complexes between chitosan and Eudragit® L 100.

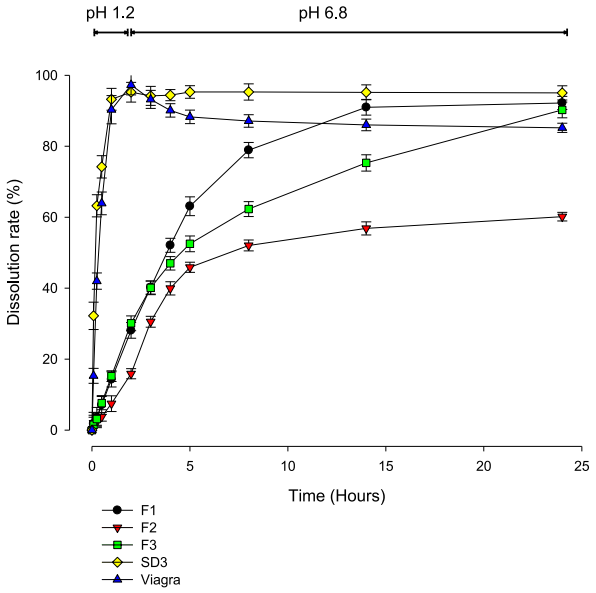

Fig. 6. Comparative release profiles of SIL-loaded SD3 and polymeric-based matrix tablets via polyelectrostatic interaction of differently charged polymers (n = 3).

3.5. Charge density

To elucidate the mechanism of polyelectrostatic interactions related to the drug release behaviors, the changes of charge density of Soluplus®-based SD3 and polymeric-based matrix tablets in different media, deionized water, gastric fluid (pH 1.2) and intestinal fluid (pH 6.8) are shown in Fig. 7. Due to the pH-dependent and low water solubility of native chitosan and Eudragit® L 100, we found that there was no significant difference in the charge density between different formulations in DW. Conversely, in pH 1.2, there was a significant increase in the density of the charge of chitosan-based formulations, such as F1 and F3, which was significantly higher than SD3 and F2. A major reason for this could be the protonation of amino groups (NH_3^+) in chitosan in pH 1.2 solution, resulting in a higher charge density and a more rapid swelling of chitosan [31]. As a result, the drug release from F1 and F3 matrix tablet was hampered and

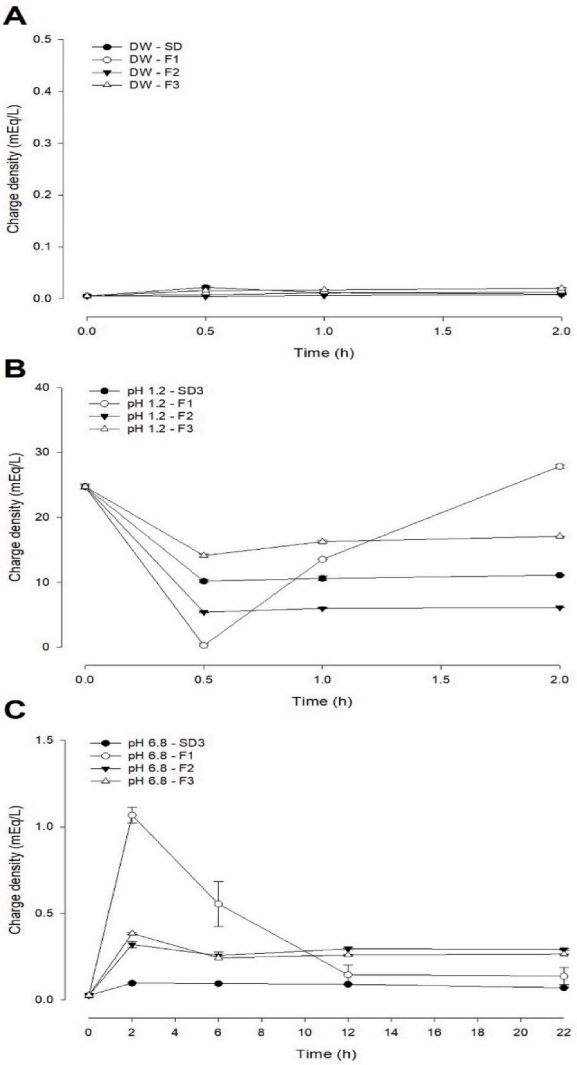

Fig. 7. The changes of charge density of Soluplus®-based SD3 and polymeric-based matrix tablets in different media (A) deionized water, (B) gastric fluid (pH 1.2) and (C) intestinal fluid (pH 6.8) (n = 3)

significantly lower than in SD3 as mentioned in the dissolution study owing to the swelling of chitosan at low pH 1.2 solution. However, when the pH was shifted to 6.8 solution, the NH_3^+ groups of chitosan were deprotonated, resulting in a reduction in charge density. The charge density of F1 at pH 6.8 solution dramatically decreased from 1.1 mEq/L to 0.2 mEq/L. Consequently, the swellability of chitosan was weakened, allowing more water to infiltrate in matrix tablet (F1), resulting in faster drug release. As compared to SD3, the incorporation of Eudragit® L 100 elevated the charge density of the solution after switching into pH 6.8 due to activation of anionic charges of Eudragit® L 100 in the pH above 6.0. Interestingly, the combination of chitosan and Eudragit® L 100 in F3 not only maintained the charge density same as in F2, but also was higher than F1 after 12 h in pH 6.8. When the pH was switched from 1.2 to 6.8, chitosan could interact electrostatically with Eudragit® L 100, which is helpful in retarding the precipitation process of chitosan and reducing the interaction between cationic drug and anionic polymer, thereby allowing the drug to be released in a controlled manner. Collectively, mechanistic understanding of the designed matrix tablet containing SIL-loaded SDs simultaneously controlling drug solubility and release rate via polyelectrostatic molecular interaction is shown in Fig. 8.

4. Conclusion

In this work, we successfully improved the dissolution rate and controlled the pH-independent release manner of SIL using Soluplus®-based SDs and polyelectrostatic complexes of chitosan and Eudragit® without showing drug recrystallization or precipitation. The preparation of SIL-loaded SDs were executed by the solvent evaporation method with different polymeric carriers. Among them, the dissolution enhancement of SIL-loaded SDs indicated that Soluplus® was the best polymeric carrier with an increase of dissolution

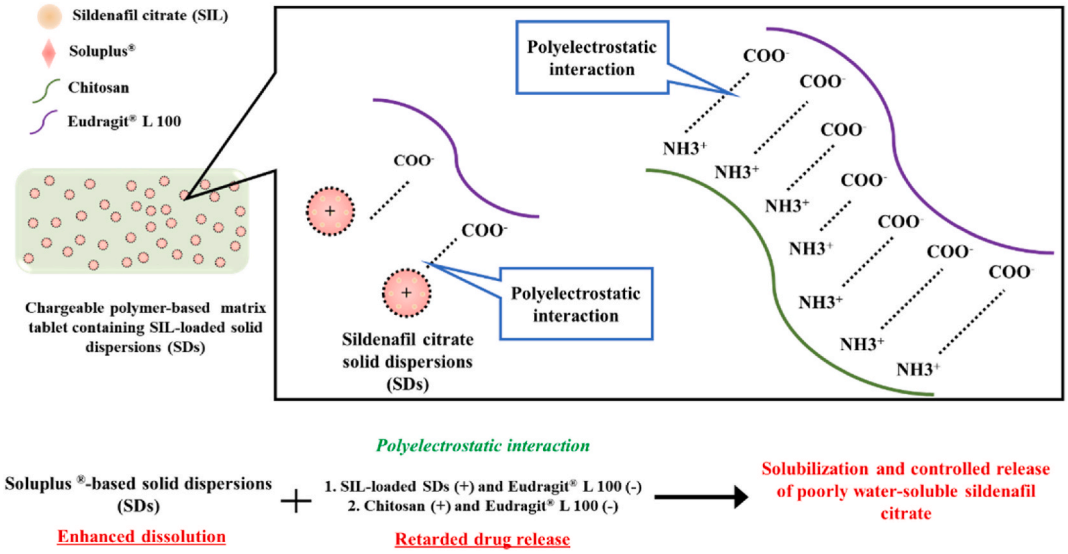

Fig. 8. Mechanistic understanding of the designed matrix tablet containing SIL-loaded SDs simultaneously controlling drug solubility and release rate via polyelectrostatic molecular interaction.

rate approximately two times compared with pure SIL at pH 6.8. The characterization of SIL-loaded SDs showed that SIL was well dispersed in SDs in an amorphous form. The controlled release of SIL-loaded SDs was obtained with the polyelectrostatic interaction between chitosan and Eudragit® L 100 in matrix tablet. This interaction remained the charge density after pH switching from 1.2 to 6.8, retarding the release rate of SIL. As a result, the mixture of chitosan and Eudragit® L 100 matrix tablet containing Soluplus®-based SDs showed the optimal release profile over 24 h. Thus, this SIL-loaded matrix tablet could be considered as an alternative to substitute three-times a day commercial tablet for better patient centricity and adherence. However, this study did not evaluate the *in vivo* pharmacokinetic performance of our matrix tablet. Further studies are needed to assess the bioavailability and toxicity of SIL in this new dosage form for treating pulmonary arterial hypertension.

Data availability statement

Data will be made available on request.

CRediT authorship contribution statement

Ju-Hyeong Woo: Writing – original draft, Visualization, Validation, Resources, Methodology, Investigation, Data curation. **Hai V. Ngo:** Writing – review & editing, Visualization, Validation, Resources, Formal analysis, Data curation. **Hy D. Nguyen:** Writing – review & editing, Visualization, Validation, Data curation. **Myung-Chul Gil:** Visualization, Validation, Data curation. **Chulhun Park:** Visualization, Validation, Data curation. **Jun-Bom Park:** Visualization, Data curation. **Jing-Hao Cui:** Validation, Data curation. **Qing-Ri Cao:** Validation, Data curation. **Beom-Jin Lee:** Visualization, Validation, Supervision, Project administration, Methodology, Investigation, Funding acquisition, Formal analysis, Data curation, Conceptualization.

Declaration of competing interest

The authors declare that they have no known competing financial interests or personal relationships that could have appeared to influence the work reported in this paper.

Acknowledgements

This work was supported by a grant from the National Research Foundation of Korea (NRF) funded by the Ministry of Science and ICT (2020R1A2C2008307), Republic of Korea. We would like to thank Ajou University–Central Laboratory for the use of instruments: FT-IR, PXRD, FE-SEM, and DSC. The SIL-loaded SDs will be used to compare with SIL-loaded fattigated nanoparticles for pharmaceutical advantages of solubilization and controlled release of poorly water-soluble drugs.

References

[1] D. Montani, S. Günther, P. Dorfmüller, F. Perros, B. Girerd, G. Garcia, X. Jaïs, L. Savale, E. Artaud-Macari, L.C. Price, M. Humbert, G. Simonneau, O. Sitbon, Pulmonary arterial hypertension, Orphanet J. Rare Diseases 8 (2013), 97-97.

[2] S.-J. Chen, J.-H. Huang, W.-J. Lee, M.-T. Lin, Y.-S. Chen, J.-K. Wang, Diagnosis of pulmonary arterial hypertension in children by using cardiac computed tomography, Korean J. Radiol. 20 (2019) 976–984.

[3] C.F. Barnett, R.F. Machado, Sildenafil in the treatment of pulmonary hypertension, Vasc. Health Risk Manag. 2 (2006) 411–422.

[4] A. Pranitha, P.K. Lakshmi, Effect of pH on weakly acidic and basic model drugs and determination of their ex vivo transdermal permeation routes, Brazilian J Pharm Sci 54 (2018), e00070, https://doi.org/10.1590/s2175-97902018000200070.

[5] M.M. Moschos, E. Nitoda, Pathophysiology of visual disorders induced by phosphodiesterase inhibitors in the treatment of erectile dysfunction, Drug Des. Dev. Ther. 8 (2016) 3407–3413.

[6] T.T.-D. Tran, P.H.-L. Tran, B.-J. Lee, Dissolution-modulating mechanism of alkalizers and polymers in a nanoemulsifying solid dispersion containing ionizable and poorly water-soluble drug, Eur. J. Pharm. Biopharm. 72 (2009) 83–90.

[7] J.-B. Park, C. Park, Z.Z. Piao, H.H. Amin, N.M. Meghani, P.H. Tran, T.T. Tran, J.-H. Cui, Q.-R. Cao, E. Oh, pH-independent controlled release tablets containing nanonizing valsartan solid dispersions for less variable bioavailability in humans, J. Drug Deliv. Sci. Technol. 46 (2018) 365–377.

[8] P. Sanphui, S. Tothadi, S. Ganguly, G.R. Desiraju, Salt and cocrystals of sildenafil with dicarboxylic acids: solubility and pharmacokinetic advantage of the glutarate salt, Mol. Pharm. 10 (2013) 4687–4697.

[9] K.M. Hosny, H.A. Mosli, A.H. Hassan, Soy polysaccharide as a novel superdisintegrant in sildenafil citrate sublingual tablets: preparation, characterization, and in vivo evaluation, Drug Des. Dev. Ther. (2015) 465–472.

[10] J.S. Kim, F.u. Din, S.M. Lee, D.S. Kim, M.R. Woo, S. Cheon, S.H. Ji, J.O. Kim, Y.S. Youn, K.T. Oh, Comparison of three different aqueous microenvironments for enhancing oral bioavailability of sildenafil: solid self-nanoemulsifying drug delivery system, amorphous microspheres and crystalline microspheres, Int. J. Nanomed. (2021) 5797–5810.

[11] S. Sawatdee, H. Phetmung, T. Srichana, Sildenafil citrate monohydrate–cyclodextrin nanosuspension complexes for use in metered-dose inhalers, Int. J. Pharm. 455 (2013) 248–258.

[12] M.F. Aldawsari, M.K. Anwer, M.M. Ahmed, F. Fatima, G.A. Soliman, S. Bhatia, A. Zafar, M.A. Aboudzadeh, Enhanced dissolution of sildenafil citrate using solid dispersion with hydrophilic polymers: physicochemical characterization and in vivo sexual behavior studies in male rats, Polymers 13 (2021) 3512.

[13] K.M. Hosny, K.M. El-Say, O.A. Ahmed, Optimized sildenafil citrate fast orodissolvable film: a promising formula for overcoming the barriers hindering erectile dysfunction treatment, Drug Deliv. 23 (2016) 355–361.

[14] A. Sachan, K. Tripathi, P. Sachan, S. Gangwar, Fabrication and characterization of compressed solid dispersion based fast dissolving tablets of sildenafil citrate, Int. J. Pharmaceut. Sci. Rev. Res. 30 (2015) 98–104.

[15] J. Niu, H.-Z. Lin, S.-G. Jiang, X. Chen, K.-C. Wu, Y.-J. Liu, S. Wang, L.-X. Tian, Comparison of effect of chitin, chitosan, chitosan oligosaccharide and N-acetyl-d-glucosamine on growth performance, antioxidant defenses and oxidative stress status of Penaeus monodon, Aquaculture 372 (2013) 1–8.

[16] H. Park, K. Park, D. Kim, Preparation and swelling behavior of chitosan-based superporous hydrogels for gastric retention application, J. Biomed. Mater. Res. 76A (2006) 144–150.

[17] J. Ostrowska-Czubenko, M. Gierszewska, M. Pieróg, pH-responsive hydrogel membranes based on modified chitosan: water transport and kinetics of swelling, J. Polym. Res. 22 (2015) 153.

[18] V.K. Nikam, K. Kotade, V. Gaware, R. Dolas, K. Dhamak, S. Somwanshi, A. Khadse, V. Kashid, Eudragit a versatile polymer: a review, Pharmacologyonline 1 (2011) 152–164.

[19] G. Jin, H.V. Ngo, J. Wang, J.-H. Cui, Q.-R. Cao, C. Park, B.-J. Lee, Electrostatic molecular effect of differently charged surfactants on the solubilization capacity and physicochemical properties of salt-caged nanosuspensions containing pH-dependent and poorly water-soluble rebamipide, Int. J. Pharm. 619 (2022), 121686.

[20] U.R. Mallu, K.H. Reddy, V. Bobbarala, S. Penumajji, RP-HPLC method development and validation for determination of dissolution and assay of sildenafil citrate tablets, J. Pharm. Res. (2010) 631–635.

[21] P. Melnikov, P.P. Corbi, A. Cuin, M. Cavicchioli, W.R. Guimarães, Physicochemical properties of sildenafil citrate (Viagra) and sildenafil base, J. Pharmaceut. Sci. 92 (2003) 2140–2143.

[22] M. Fukuda, N.A. Peppas, J.W. McGinity, Properties of sustained release hot-melt extruded tablets containing chitosan and xanthan gum, Int. J. Pharm. 310 (2006) 90–100.

[23] M. Sharma, V. Sharma, A.K. Panda, D.K. Majumdar, Development of enteric submicron particle formulation of papain for oral delivery, Int. J. Nanomed. 6 (2011) 2097.

[24] M.A. Abbasi, S. Ahmad, A.-u. Rehman, S. Rasool, K.M. Khan, M. Ashraf, R. Nasar, T. Ismail, Sulfonamide derivatives of 2-amino-1-phenylethane as suitable cholinesterase inhibitors, Trop. J. Pharmaceut. Res. 13 (2014) 739–745.

[25] J. Bhagyasree, H.T. Varghese, C.Y. Panicker, J. Samuel, C. Van Alsenoy, K. Bolelli, I. Yildiz, E. Aki, Vibrational spectroscopic (FT-IR, FT-Raman, 1H NMR and UV) investigations and computational study of 5-nitro-2-(4-nitrobenzyl) benzoxazole, Spectrochim. Acta Mol. Biomol. Spectrosc. 102 (2013) 99–113.

[26] N.-Y. Topsøe, Characterization of the nature of surface sites on vanadia-titania catalysts by FTIR, J. Catal. 128 (1991) 499–511.

[27] H.-J. Butt, Measuring electrostatic, van der Waals, and hydration forces in electrolyte solutions with an atomic force microscope, Biophys. J. 60 (1991) 1438–1444.

[28] S.-H. Park, M.-K. Chun, H.-K. Choi, Preparation of an extended-release matrix tablet using chitosan/Carbopol interpolymer complex, Int. J. Pharm. 347 (2008) 39–44.

[29] Y. Shao, L. Li, X. Gu, L. Wang, S. Mao, Evaluation of chitosan–anionic polymers based tablets for extended-release of highly water-soluble drugs, Asian J. Pharm. Sci. 10 (2015) 24–30.

[30] P. Thapa, D.H. Choi, M.S. Kim, S.H. Jeong, Effects of granulation process variables on the physical properties of dosage forms by combination of experimental design and principal component analysis, Asian J. Pharm. Sci. 14 (2019) 287–304.

[31] R. Miranda, R. Nicu, I. Latour, M. Lupei, E. Bobu, A. Blanco, Efficiency of chitosans for the treatment of papermaking process water by dissolved air flotation, Chem. Eng. J. 231 (2013) 304–313.